J. ISSS Vol. 3 No. 1, pp.18-27, March 2014.
REGULAR PAPER

Low Frequency Vibration Energy Harvesting using Arrays of PVDF Piezoelectric Bimorphs

Rammohan S.[a], Ramya C. M.[c], Jayanth Kumar S.[b], Anjana Jain[b], Rudra Pratap[a,c]
[a] Department of Mechanical Engineering, Indian Institute of Science, Bangalore 560012
[b] National Aerospace Laboratories, Bangalore 560017
[c] Centre for Nano Science and Engineering, Indian Institute of Science, Bangalore 560012
Corresponding author: rammohan@mecheng.iisc.ernet.in

Keywords:
Energy harvesting, piezoelectric converter, array of bimorphs, electromechanical coupling coefficient, PVDF.

Abstract

Power harvesters based on the piezoelectric effect are more promising in harnessing energy from ambient vibrations. In this paper, piezoelectric bimorph resonators in the form of Polyvinylidinefluoride (PVDF) cantilevers are studied and used in an array with optimal terminal combination for maximizing the power generated from low frequency vibrations. The thickness of the passive sandwich layer and the poling direction in each film are observed to be crucial in determining the total power generated from the PVDF bimorph. Experimentally, bimorph cantilevers made of 55 μm thick PVDF film and sized to resonate between 30 to 40 Hz are used in similarly poled as well as oppositely poled configurations and their output measured as voltage across a 1 MΩ load resistance. The similarly poled bimorph outperforms the oppositely poled configuration by more than doubling the output voltage. Further enhancement in the output is observed by introducing a sandwich layer of 50 μm thick copper foil between the two similarly poled PVDF layers. Experiments with three such devices connected in parallel in an array and resonating at 33 Hz with an input acceleration of 0.8 g results in 2.8 μW power generation. This result shows the promise of PVDF as a candidate material for energy harvesting resonators despite its low electromechanical coupling coefficient (k_e). Low cost and ease of production may be especially attractive for PVDF.

1. Introduction

Interest in energy harvesting from ambient vibrations has increased several folds in the recent years. Energy harvested from vibrations is invaluable for devices operating in remote environments. The advent of low power consuming electronics facilitates the ability to supply the necessary energy for operation from the energy in the ambience. Furthermore, inconsiderable advancement in the battery energy densities over the past two decades compels us to search for alternatives to the battery technologies. Smart systems such as structural health monitoring sensors and wireless sensing nodes can be powered by the energy from the ambient motion eliminating the need for periodic battery replacements [Beeby *et al*. 2006], [Roundy *et al.* 2003]. The necessary power for operation can be delivered by the harvester exploiting

Available online at www.isssonline.in/journal/03paper03.pdf Paper submitted on December 31, 2013. Accepted on May 31, 2014.

electromagnetic, electrostatic or piezoelectric effect.

In electromagnetic and piezoelectric conversion mechanisms, the required voltages are generated directly while in electrostatic generators, the conversion process is initiated by a separate voltage source. Electromagnetic generators are suitable for scavenging energy at high frequencies, while piezoelectric harvesters can outperform the electromagnetic generators at low frequencies [Mitcheson *et al.* 2006]. The normalized power from the piezoelectric harvesters within 100 Hz is comparable to that of the electromagnetic harvesters. Additionally, the volume occupied by the piezoelectric harvesters is smaller than the electromagnetic generators for a given normalized power density[Beeby *et al.* 2007]. Piezoelectric conversion is, therefore, a better mechanism to scavenge energy at frequencies below 100 Hz. However, not many piezoelectric materials are suitable for low frequency resonator designs [Jeon *et al.* 2005]. A harvester configuration as a cantilever bimorph can reduce the natural frequency. This results in piezoelectric cross coupling between the stress and the polarization directions which is smaller than the direct coupling. Nevertheless, a cantilever configuration allows stress amplification for a given excitation and thus competes with the direct coupling configurations of the harvesters [Baker *et al.* 2005]. Polyvinylidinefluoride (PVDF) is selected here as the piezoelectric material for harvesters owing to its low elastic stiffness allowing the design of resonators with the fundamental mode of vibration below 100Hz.

The cantilever configuration of a piezoelectric harvester with a single layer of piezoelectric material is called a *unimorph* and that with two layers is called a *bimorph*. A bimorph can further have two variants depending on the direction of poling in the two piezoelectric layers. A vibrating bimorph with alternating stresses in the two layers imposes a series combination of the layers when poling is opposite and a parallel combination when poling is similar [Steven *et al.* 2007]. A generic design methodology of a piezoelectric bimorph is described in section 2. Electromechanical coupling coefficient, k_e, is an indicator of the transduction strength in a piezoelectric harvester. PVDF bimorph with a low k_e (<0.1) is a weak harvester. In this paper, observations specific to low k_e bimorphs are made and efficient schemes of combining the output are elucidated. It is analytically noticed that a bimorph with similar poling in both the films results in more power than that with opposed poling. Moreover, bimorphs with weak k_e tend to show constancy in the current generated over practical range of load resistances resulting in power generation governed solely by the variation in the voltage. However, this trend is not followed at very large load resistances (>100 MΩ), but for practical resistances up to 2 MΩ power increases with the increase in the load resistance. These remarks are experimentally corroborated using PVDF bimorphs made of 55 μm thick film and designed to resonate at 32 Hz as described in section 4. Power output from a single bimorph for 0.8 g input resonating at 32 Hz varies from 0.9 to 1.4 μW across 1 MΩ load depending on the damping ratio. Power density of a single PVDF bimorph is estimated to be 12 μW/cm^3. Although power density from a single harvester is small, output from an array of bimorphs is observed to be sufficient to drive a rectifier circuit and have a net positive power delivered across a load resistance. Conclusions in section 5 highlight the characteristics of the designed bimorphs and the optimum scheme for combining the individual output to increase the total power generated.

2. Design and analysis

2.1 Piezoelectric Constitutive Relations

Electromechanical modeling of a piezoelectric beam is carried out using the isothermal stress-charge form of piezoelectric constitutive equations:

$$T_I = c_{IJ}^E S_J - e_{iI} E_i \quad (1)$$

$$D_i = e_{iJ} S_J + \varepsilon_{ij}^S E_j \quad (2)$$

Here, T and S are stress and strain in Voigt's notation with subscripts I and J varying from 1 to 6. Electric field E and electric displacement D have subscripts i and j varying from 1 to 3. Elastic stiffness at constant electric field and relative permittivity at constant strain are denoted by c^E and ε^S respectively. Piezoelectric stress coefficients forming a third order tensor are condensed due to the crystal symmetry and denoted by e.

2.2 Piezoelectric Bimorph in Series Configuration

Schematic of a bimorph in series configuration is shown in figure 1 indicating the direction of poling and the electric field. Power from the vibrating bimorph is delivered across the load resistance, R_l.

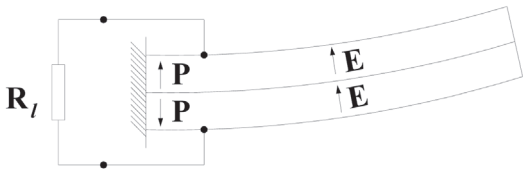

Figure 1: Schematic of Series Bimorph

Bimorph with electrodes on either side of the piezoelectric layers results in non-zero electric field in the thickness direction. Transverse vibrations of the bimorph result in significant bending stresses along the longitudinal direction of the beam simplifying the stress-charge relations. Besides, *mm2* symmetry in PVDF results in the following reduced form of equations (1) and (2).

$$T_1 = c_{11}^E S_1 - e_{31} E_3 \tag{3}$$

$$D_3 = e_{31} S_1 + \varepsilon_{33}^S E_3 \tag{4}$$

2.2.1 Electric field and Strain

The arrangement of the electrodes defines the equipotential surfaces for potential distribution function φ. Potential difference between the two electrodes in a single layer is denoted by v_p. Potential distribution along the thickness is assumed to be linear with *z* and is given by:

$$\varphi_z = \frac{v_p(t)}{c} z \tag{5}$$

Hence, the electric field in *z* direction is given by:

$$\underline{E} = -\nabla\varphi \Rightarrow E_3(t) = -\frac{v_p(t)}{c} \tag{6}$$

The thickness of each piezoelectric layer is denoted by *c* as shown in figure 2. Width *b* and length *l* of the electrode are assumed to span over the entire surface of the beam.

Figure 2: Equipotential surfaces and axes conventions.

As per the axes conventions illustrated in figure 2, the strain in *x* – direction (*x* is 1 in the indicial notation) for small slopes is related to the relative displacement $u_r(x, t)$ of the beam by:

$$S_1 = -z u_{r,11} \tag{7}$$

Using equations (6) and (7) the constitutive equations for the vibrating bimorph with *v* as the potential across the load resistance are rewritten as

$$T_1 = -c_{11}^E z u_{r,11} + e_{31} \frac{v(t)}{2c} \tag{8}$$

$$D_3 = -e_{31} z u_{r,11} - \varepsilon_{33}^S \frac{v(t)}{2c}. \tag{9}$$

2.2.2 Bending Moment

The bending moment, M_b, at a given cross section along the beam is given by:

$$M_b(x,t) = -\int_{-c}^{c} T_1 b z dz \tag{10}$$

Substituting T_1 from equation (8) into the above equation results in the bending moment in terms of curvature and piezoelectric stress coupling:

$$M_b(x,t) = \frac{2}{3} b c^3 c_{11}^E u_{r,11} - \frac{1}{2} e_{31} v(t) b c. \tag{11}$$

The second term in equation (11) is obtained by performing integration over the individual layer thicknesses considering the poling and electric field directions in the respective layers.

2.2.3 Enclosed Charge

The charge in between the electrodes is obtained from the Gauss's law by performing integration over the electrode area Γ as follows,

$$Q = \int_{\Gamma} \underline{D} \bullet d\underline{\Gamma} = \int_{\Gamma} D_3 dy dx \tag{12}$$

Substituting equation (9) into equation (12) results in the expression for enclosed charge:

$$Q = -e_{31} z b u_{r,1} - \varepsilon_{33}^S b l_e \frac{v(t)}{2c} \tag{13}$$

2.2.4 Equations of Motion

The equations of motion are coupled between the potential *v* across the load resistance and the

relative displacement u_r of the beam. One coupled equation of motion is obtained from equation (13). The second equation is derived from the equilibrium of the differential element of the vibrating bimorph. The force balance equation in terms of the equivalent mass per unit length (ρA) and the damping coefficient (C_a) for a given ground displacement u_g is

$$M_{b,11} + C_a u_{r,t} + \rho A u_{r,tt} = -\rho A u_{g,tt} \quad (14)$$

Before substituting the bending moment from equation (11) into equation (14), the second term in the bending moment expression is multiplied by the Heaviside step function, thus introducing the electromechanical coupling. Employing the separation of variables by expressing the relative displacement u_r as a product of spatial variation $\phi(x)$ and temporal variation $r(t)$, the partial differential equation is transformed to an ordinary differential equation. Invoking the orthogonality of the mode shapes, the equations of motion for a bimorph of mass M, layer capacitance C_p and coupling coefficient ω_n are given by:

$$\ddot{r}_n(t) + 2\zeta_n \omega_n \dot{r}_n(t) + \omega_n^2 r_n(t) - \frac{\theta}{M} v(t) = -a_f \quad (15)$$

$$\frac{C_p}{2}\dot{v}(t) + \frac{1}{R_l} v(t) + \theta \dot{r}_n(t) = 0 \quad (16)$$

where,

$$\omega_n = a_{L_n}^2 \frac{c}{\sqrt{3}l^2}\sqrt{\frac{c_{11}^E}{\rho}} \quad (17)$$

$$\theta = \frac{1}{2} e_{31} bc \psi_{,x}(l); \qquad C_p = \frac{\varepsilon_{33}^S bl}{c} \quad (18)$$

$$a_f = \frac{1}{l} u_{g,tt} \int_0^l \psi(x)dx \quad (19)$$

$$\psi(x) = \cos ax - \cosh ax - \left[\frac{\cos a_L + \cosh a_L}{\sin a_L + \sinh a_L}\right](\sin ax - \sinh ax) \quad (20)$$

The coefficient a_{Ln} in $\dot{u}_n$ for n^{th} mode is obtained from the transcendental equation for a cantilever as given by:

$$\cosh a_{L_n} \cos a_{L_n} + 1 = 0$$

It is to be noted that equation (16) is obtained by differentiating the charge in equation (13) with time and equating it to the current flowing into the load resistance [Sodano *et al*. 2004], [Jiang *et al*. 2005].

2.3 Piezoelectric Bimorph in Parallel Configuration

When the poling in the two piezoelectric layers is alike then the layers have to be connected in parallel as shown in figure (3). The formulation described in section 2.2 holds even in the parallel configuration. Equations of motion for the bimorph in this configuration are also as described in equations (15) and (16). However, the coefficients θ and C_p described in equation (18) are to be multiplied by 2 before substituting into the equations of motion. The reason for multiplying 2 in the case of coupling coefficient θ is that the net electric field in parallel configuration is twice of that in the series configuration. Also, the effective capacitance of the bimorph is double the layer capacitance as the two films are in parallel. Moreover, a passive sandwich layer of thickness a and elastic modulus c_s between the two layers modifies the bending moment as

$$M_b(x,t) = \frac{b}{12}\left\{(8c^3 - a^3)c_{11}^E + c_s a^3\right\} u_{r,xx} - e_{31} v(t) b(c + \frac{a}{2})\{H(x) - H(x-l)\} \quad (21)$$

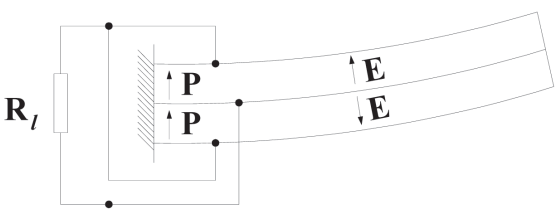

Figure 3: Schematic of Parallel Bimorph

3. Complex Harmonic Response

Steady state frequency response for voltage and power are obtained by assuming a complex forcing function. The linear differential equations are solved by defining the complex harmonic response functions as:

$$a_f(t) = A_f e^{j\omega t} \qquad r(t) = \mathrm{Re}^{j\omega t} \qquad v(t) = Ve^{j\omega t}$$

Substituting the above expressions in equations of motion (15) and (16), the complex

harmonic voltage, assuming the first mode operation, is obtained as follows.

$$V = \frac{\alpha\beta k_e^2}{\left(\alpha\left(1+k_e^2-\beta^2\right)+2\zeta\right)\beta + j\left(\beta^2\left(1+2\alpha\zeta\right)-1\right)} \frac{MA_f}{\theta} \tag{22}$$

where,

$$\alpha = C_p R_l \omega_n; \qquad \beta = \frac{\omega}{\omega_n}; \qquad k_e^2 = \frac{\theta^2}{M\omega_n^2 C_p}; \tag{23}$$

The complex form of the current flowing into the load resistance is obtained from Ohm's law:

$$i = \frac{V}{R_l} \tag{24}$$

The power P delivered at the load resistance is obtained from the product of rms values of voltage and current:

$$P = \frac{V_{rms}^2}{R_l} = \frac{V^2}{2R_l} \tag{25}$$

The power output given by equation (25) is maximized with respect to load resistance and the optimum load resistance [duToit *et al.* 2005], [Shu *et al.* 2006] corresponding to the maximum power generation is given by:

$$R_{op} = \frac{2\zeta}{C_p\omega\sqrt{k_e^4+4\zeta^2}} \tag{26}$$

For small values of electromechanical coupling coefficient k_e and the piezo layer capacitance C_p, the optimum load resistance is large as it is inversely proportional to C_p. Operating at such large optimum load resistance is not always practical. However, it will be evident from equation (27) that in weak k_e devices, the current at resonance is independent of load resistance. From equations (22) and (24), the complex harmonic current response at resonance can be approximated as

$$i \cong \frac{C_p\omega_n k_e^2}{2\zeta\theta} MA_f \tag{27}$$

It is evident from the above equation that the current from the bimorph with weak k_e is independent, at least for most practical values, of load resistance and hence, bimorphs can be combined in parallel for increasing the total power generated. These observations are verified experimentally by fabricating weak k_e bimorphs made of PVDF film as discussed in the next section.

4. Experimental Results

4.1 PVDF Bimorph

Series and parallel configurations of bimorphs are fabricated with 55 μm thick PVDF film. Conductive adhesive is used to glue the two layers integrated with electrodes. Length of the bimorphs is set to 30 mm to obtain the fundamental resonance frequency below 100 Hz as the resonator represents a composite beam. Density, elastic modulus, piezoelectric strain coefficient, and relative permittivity for the selected PVDF film used in the simulations are 1750 kg/m^3, 2.8 GPa, 8 pC/N, and 10 respectively. Bimorphs are subjected to a sine sweep from 10 Hz to 150 Hz for various input accelerations up to 0.8 g. The experimental setup is schematically shown in figure 4.

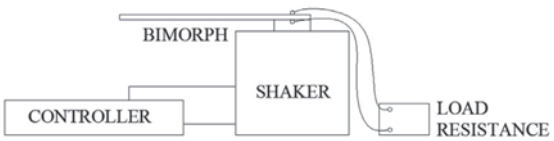

Figure 4: Schematic of experimental test setup. The bimorph is driven by the shaker, and controller. Power developed by bimorph is measured across the load resistance.

The predicted first mode resonance frequencies, depending on the dimensions for series and parallel bimorphs, are 53.6 Hz and 71.1 Hz; and experimentally observed values are 54.5 Hz and 71.0 Hz, respectively. The voltage output from these devices for 0.7 g input is shown in figure 5. It

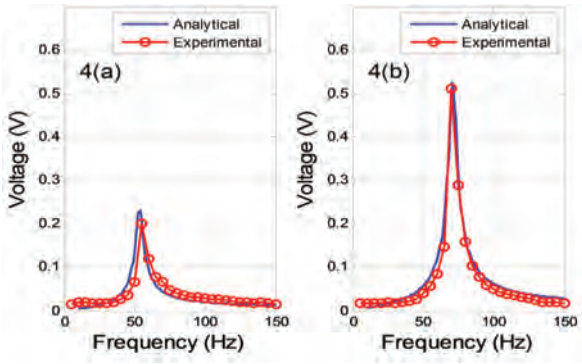

Figure 5: Voltage output from PVDF bimorph for R_l = 1 MΩ and 0.7 g input acceleration (a) in series configuration (b) in parallel configuration.

is evident from the plot that the bimorph with parallel configuration results in higher voltage, increasing the total power. Analytically, voltage is obtained from the equations (18) and (22).

Additionally, another set of bimorph cantilevers of 30 mm length, 10 mm width, and 0.2 mm thickness resonating at 32 Hz with 0.5 g input resulted in 0.61 V across 1 MΩ load resistance while the bimorphs with opposed poling read only 0.28V. Hence, parallel configuration of the bimorph is more effective for a given volume of the material. Moreover, it can be inferred from equation (21) that sandwiching a passive elastic layer enhances the bending stresses and hence, the potential developed. A copper foil of thickness 50 μm between the two piezo layers results in k_e = 0.02. This increase in k_e (equation (23)) with the addition of copper foil is attributed to considerable increase in the index of coupling θ, compared to the increase in M, and ω_n, as C_p is constant. Unless otherwise stated, the subsequent discussion on bimorph refers to the parallel configuration of the harvester with sandwiched copper foil.

Simulations reveal the dependence of voltage and current from the bimorph on the load resistance as shown in figures 6 and 7 respectively. Voltage is observed to increase with the increase in load resistance while current is observed to be constant. The constant value of current at resonance matches with that evaluated using equation (27) within 8%. It has to be noted, however, that the current given by equation (27) is valid only at resonance.

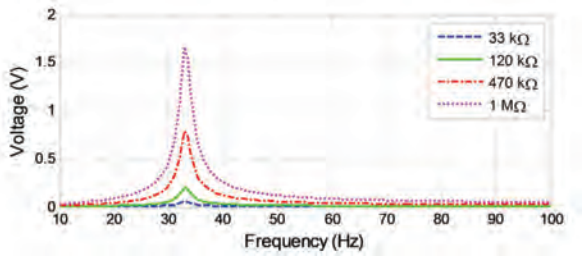

Figure 6: Voltage frequency response of bimorph for 0.8 g input

For simulations, the length, width and thickness of the bimorph are taken as 35 mm, 10 mm and 0.2 mm respectively.

Similarly the power generated is evaluated using equation (25). As the current from the bimorph is constant, the power generated follows the

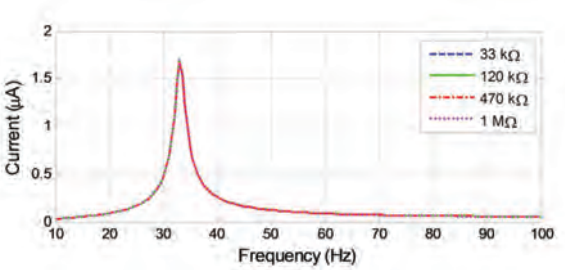

Figure 7: Current frequency response of bimorph for 0.8 g input

variation in voltage. Power delivered increases with the load resistance as shown in figure 8 which is similar to the voltage variation. Simulations reveal that power output close to 1.4 μW is delivered across 1 MΩ load.

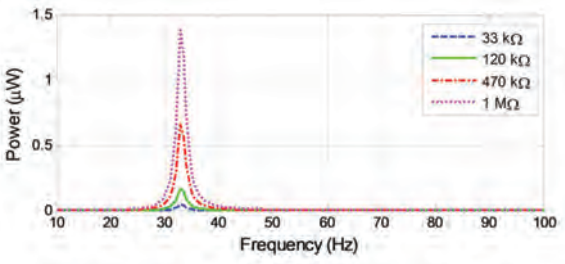

Figure 8: Power frequency response of bimorph for 0.8 g input

The response of the parallel configuration bimorph of length 35 mm for a 0.5 g sine sweep at 3.2 oct/min from 10 Hz to 100 Hz is depicted in figure 9. Prediction matches with the experimental results within 15% over the frequency range from 20 Hz to 100 Hz. Furthermore, it can be noticed from the plot that the voltage output at resonance (34 Hz) is 1.3 V.

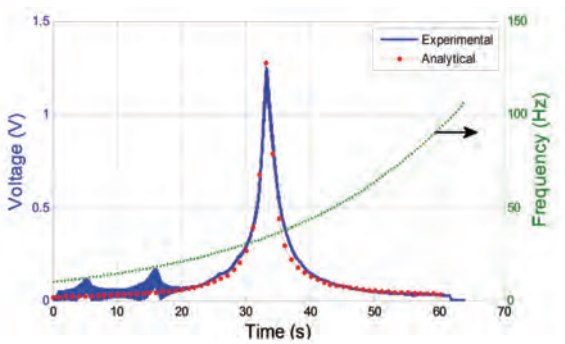

Figure 9: Voltage response of PVDF bimorph for R_l = 1 MΩ during vibration test. Also shown is the variation in the excitation frequency with time. One can read the voltage at a particular frequency by matching the corresponding time of occurrence.

Voltages measured at resonance from this device for an acceleration input of 0.8 g across 1 MΩ and 2 MΩ load resistances are 1.76 V and 3.21 V. The estimated currents into the two resistors are thus 1.77 μA and 1.60 μA. These values match with calculated current from equation (27) within 8%. It is noticed from figure 10 (equation (24)) that the current output remains constant for 1 MΩ and 2 MΩ load resistances.

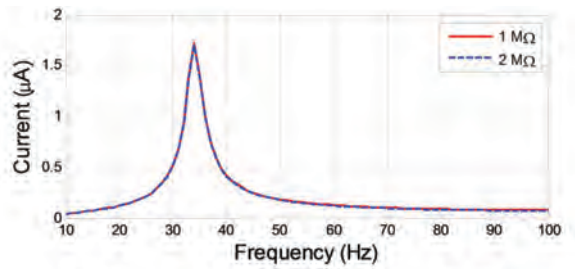

Figure 10: Harmonic Response of Current for 0.8 g acceleration

4.2 Array of PVDF Bimorphs

The PVDF bimorph modeled here as a current source with the film capacitance in parallel allows connecting a set of such devices in parallel for increased total power. The open circuit voltage from five parallel bimorphs for 0.8 g input acceleration is shown in figure 11.

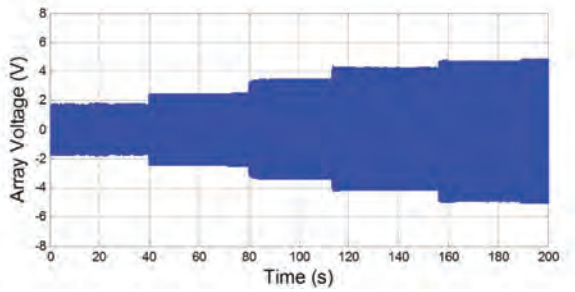

Figure 11: Open circuit array voltage from 5 PVDF bimorphs in staggered configuration activated sequentially.

Differences in the capacitances of the adjacent devices and distortion in the waveforms of the bimorphs can adversely affect the total power generated. However, given similar devices, the voltage builds linearly and hence the array of bimorphs can favorably be used to drive the necessary regulating electronics and obtain a net positive power. The AC output from the array of three devices under a sinusoidal excitation at 33 Hz is rectified and filtered using a 47 μF capacitor. The plot of voltage build-up is shown in figure 12. Power is estimated by connecting a known load resistance across the terminals.

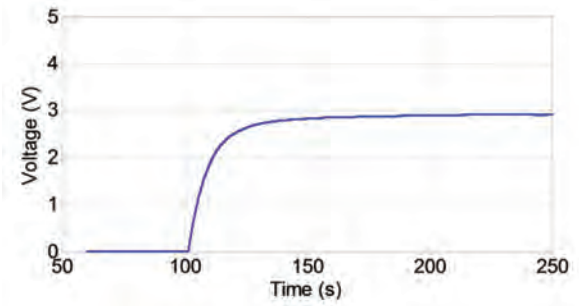

Figure 12: Rectified output from an array of 3 bimorphs.

The rectified voltage output from an array of three parallel bimorphs resonating at 33 Hz for 0.8 g input loaded with 1 MΩ and 2 MΩ resistances is shown in figure 13. In steady state, the power delivered by the array excluding the losses in processing electronics (from figure 13) is 2.8 μW while the estimated power without losses is 3.2 μW for 1 MΩ load resistance.

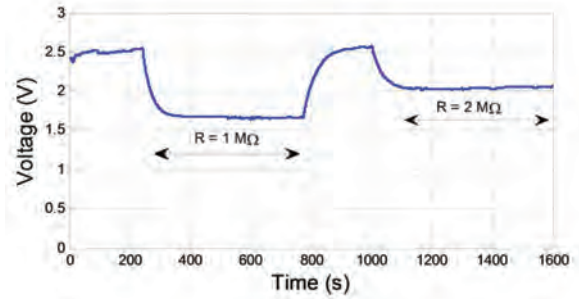

Figure 13: Rectified voltage across selected load resistances

The power output from the array has been verified by measuring both voltage and current

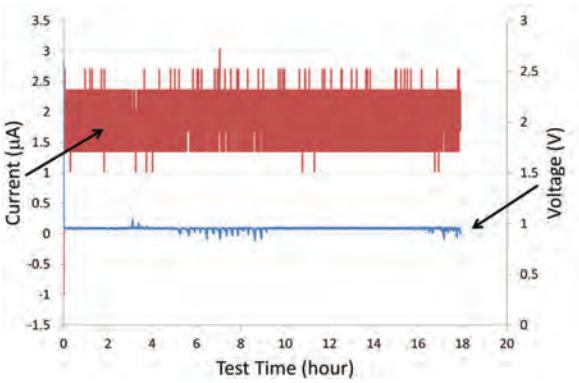

Figure 14: Current and voltage measured across 500 kΩ load.

simultaneously for a load resistance of 500 kΩ (figure 14). The expected power from the three devices is 1.5 μW while the measured power is 1.35 μW.

Rectification and regulation of the output from three parallel bimorphs is carried out using a commercially available IC [Jiang *et al*. 2010] LTC 3588-1. The output from the IC is regulated to 1.8 V as shown in figure 15, where the intermittent drop corresponds to the inadequate power input.

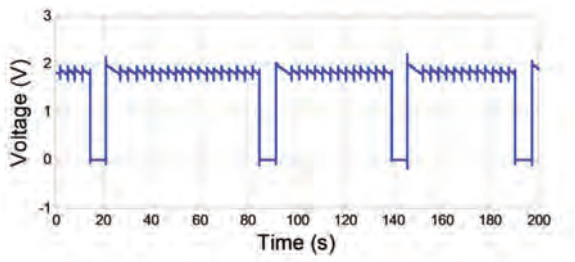

Figure 15: Regulated voltage measured using LTC-35881

Experiments corroborate that bimorphs made of weak k_e such as PVDF can be combined in parallel to increase the total power generated. In particular, the direction of poling in the two layers of the bimorph proves to be a critical factor in maximizing the power. The effectiveness of electronics is not addressed completely here, as the focus of the current work is on the method for combining bimorphs in an appropriate manner to maximize power output. The characteristic parameters of harvesters developed in various research groups are listed in the following table.

Table 1. Comparison of power developed by various low frequency harvesters

Reference	Power (μW)	Frequency (Hz)	Acceleration (m/s^2)	Power/ volume (μW/cc)
This work (PVDF)	0.9	33	7.8	12
Sodano H A *et al*, 2004 (Mide tech. - QP40N)	11.9	30	-	6.1
Lei Gu 2011 (PZT)	1500	20	3.9	93.2
Arroyo E *et al*, 2012 (PZT)	3000	130	19.6	125

5. Conclusions

Performance of weak k_e bimorph harvesters made of PVDF is addressed in this paper. The steady state voltage and power from the bimorph at its resonance are observed to be higher when the direction of poling in two films of the bimorph is alike and when an elastic layer is used between the two layers. Hence, the parallel configuration of the bimorph results in higher potential and output power. Furthermore, simulations reveal that the bimorph made of piezoelectric material with weak k_e has very high optimal load resistance making the device behave as a constant current source irrespective of the magnitude of load resistance. Average power output from a single bimorph at resonance, for 0.8 g input across 1 MΩ load, is 0.9 μW resulting in power density of 12 $\mu W/cm^3$. Designed bimorphs which are 35 mm long, 10 mm wide and 0.2 mm thick including the passive central copper foil resonate at 33 Hz. Bandwidth of the bimorph can be improved by operating the harvester in a feedback loop. However, the associated additional energy requirements have to be meticulously calculated. On the performance metric of normalized power density (power per acceleration squared per unit volume), the proposed PVDF bimorph stands at 0.2 kgs/m^3. Reported values range from 3 to 60 kgs/m^3 for strong k_e harvesters [Roundy *et al*. 2004], [Hong *et al*. 2005]. Bimorphs with weak k_e behave as constant current sources and hence, it is recommended that PVDF bimorphs be combined in parallel to form an array with increased total power demonstrating a viable energy harvesting at large scale in low frequency realms.

Acknowledgements

This work is partially supported by NPMASS grant and the facilities created by NPMASS projects at CeNSE, I.I.Sc.

References

Arroyo E, Badel A, Formosa F, Wu Y and Qiu J, 2012, Comparison of electromagnetic and piezoelectric vibration energy harvesters: Model and

experiments, *Sensors and Actuators A 183* pp 148–156.

Baker J, Roundy S and Wright P, 2005, Alternative geometries for increasing power density in vibration energy scavenging for wireless sensor networks, *Proc. 3rd Int. Energy Conversion Engineering Conf. (San Francisco, CA, Aug.)* pp 959–70.

Beeby S P, Tudor M J and White N M, 2006, Energy harvesting vibration sources for microsystems applications, *Meas. Sci. Technol.* **17** R175–R195.

Beeby S P, R N Torah, M J Tudor, P Glynne-Jones, T O'Donnell, C R Saha, S Roy, 2007 A micro electromagnetic generator for vibration energy harvesting, *J. Micromech. Microeng*, 17 1257-1265.

duToit N E, Wardle B L and Kim S G, 2005, Design considerations for MEMS-scale piezoelectric mechanical vibration energy harvesters, *Integr. Ferroelectr.*71 121–60.

Hong Y K and Moon K S, 2005, Single crystal piezoelectric transducers to harvest vibration energy, *Proc. SPIE* **6048** 60480E-1.

Jeon Y B, Sood R, Jeong J-h and Kim S G, 2005, MEMS power generator with transverse mode thin film PZT, *Sensors Actuators* A **122** 16–22.

Jiang S, Li X, Guo S, Hu Y, Yang J and Jiang Q, 2005, Performance of a piezoelectric bimorph for scavenging vibration energy, *Smart Mater. Struct.***14** 769–74.

Jiang Y, Shinon S, Hamada H, Fujita T, Higuchi K and Maenaka K, 2010, Low-frequency energy harvesting using a laminated PVDF cantilever with a magnetic mass, *PowerMEMS (Leuven)* pp 375–8.

Lei Gu, 2011, Low-frequency piezoelectric energy harvesting prototype suitable for the MEMS implementation, *Microelectronics Journal* 42, pp 277-292.

Mitcheson P D, Reilly E K, Wright P K, Yeatman E M, 2006, Transduction mechanisms and power density for MEMS inertial energy scavengers, *Proc. Power MEMS*.

Roundy S, Wright P K and Rabaye J, 2003, A study of low level vibrations as a power source for wireless sensor nodes, *Comput. Commun.* **26** 1131–44.

Roundy S and Wright P K, 2004, A piezoelectric vibration based generator for wireless electronics, *Smart Mater Struct.* **13** 1131–42.

Shu Y C and Lien I C, 2006, Analysis of power output for piezoelectric energy harvesting systems, *Smart Mater. Struct.* 15 1499–512.

Sodano H A, Park G and Inman D J, 2004, Estimation of electric charge output for piezoelectric energy harvesting, *J. Strain* **40** 49–58.

Steven R Anton and Henry A Sodano, 2007, A review of power harvesting using piezoelectric materials (2003–2006), *Smart Mater.Struct*. 16 R1-21.

Rammohan S obtained a B. Tech degree in

Mechanical Engineering from Jawaharlal Nehru Technological University, Andhra Pradesh, India in 2005. He served as design engineer in Hindustan aeronautics limited in 2005 and as scientist in Inertial systems unit of Indian space research organization from 2006 to 2011. He is currently pursuing Ph. D. in Mechanical Engineering at Indian Institute of Science. His research interests include vibration isolation, vibration control, design and analysis of electro-mechanical sensors, actuators and systems.

Ramya C M obtained her Bachelor's degree in

Electrical and Electronics Engineering from MS Ramaiah Institute of Tehnology in the year 2012. She is now working as a project assistant in the Centre for Nanoscience and Engineering, IISc. Her current research is on developing power management circuits for energy harvesting applications. Her research interests also include microelectronics and semiconductor device physics.

Jayanth Kumar S obtained M.Sc in Physics from

University of Mysore, India in the year 2005. He is currently a Ph.D. student with Mangalore University, Mangalore, India. His research interests are in development and characterization of smart materials especially for aerospace applications.

Anjana Jain has obtained Ph.D degree in Materials Science in 2002. Presently, She is a senior scientist in the Materials Science Division of National Aerospace Laboratories, Bangalore. Her fields of interest include smart materials especially development of PVDF based sensors for structural health monitoring, strain sensing and various other aerospace applications. She also has expertise in characterization of materials using X-ray diffraction technique. She is reviewer in Polymer Engineering & Science, Bulletin of Materials Science, and Surface & Coatings Technology.

Prof. Rudra Pratap received a B.Tech. degree from the Indian Institute of Technology, Kharagpur, India, in 1985, a Master's degree in mechanics from the University of Arizona, Tucson, in 1987, and a Ph.D. degree in Theoretical and Applied Mechanics from Cornell University, Cornell, NY, in 1993. He taught at the Sibley School of Mechanical and Aerospace Engineering, Cornell University during 1993–1996, prior to joining the Indian Institute of Science in 1996. He is currently a Professor with the Department of Mechanical Engineering and the Centre for Nano Science and Engineering, Indian Institute of Science Bangalore, India. His research interests include MEMS design, computational mechanics, nonlinear dynamics, structural vibration, and vibroacoustics.